Interacting topological phases in multiband nanowires

Roman M. Lutchyn[1] and Matthew P. A. Fisher[2]

[1]*Microsoft Research, Station Q, Elings Hall, University of California, Santa Barbara, CA 93106, USA*
[2]*Department of Physics, University of California, Santa Barbara, California 93106*

(Dated: compiled April 14, 2011)

We show that semiconductor nanowires coupled to an s-wave superconductor provide a playground to study effects of interactions between different topological superconducting phases supporting Majorana zero-energy modes. We consider quasi-one dimensional system where the topological phases emerge from different transverse subbands in the nanowire. In a certain parameter space, we show that there is a multicritical point in the phase diagram where the low-energy theory is equivalent to the one describing two coupled Majorana chains. We study effect of interactions as well as symmetry-breaking perturbations on the topological phase diagram in the vicinity of this multicritical point. Our results shed light on the stability of the topological phase around the multicritical point and have important implications for the experiments on Majorana nanowires.

Introduction. The possibility of realizing Majorana fermions, elusive particles that are their own anti-particles, in semiconductor nanowires coupled with an s-wave superconductor has attracted a lot of attention recently [1]. In addition to the intrinsic motivation of finding Majorana particles in nature[2], the solid-state Majoranas have additional property of fundamental physics interest: Majorana zero-energy modes emerging in topological superconductors obey non-Abelian braiding statistics[3–5] which can be exploited for quantum computation purposes [6]. The prediction of the emergence of Majorana fermions in semiconductor/superconductor heterostructures [7–10] has led to much activity aimed at detecting these exotic particles [11–15] as well as exploiting them for topological quantum computation [16–18].

There is no doubt that Majorana fermions can be realiazed in suitable mean-field models describing realistic physical systems. The existence of Majorana zero-energy modes in these system can be shown theoretically by explicitly solving the corresponding quadratic Hamiltonians [7, 9, 10, 19] or invoking topological invariants developed for noninteracting systems [20]. The situation is much more complicated, however, once interactions are included, and there are examples where interactions lead to the breakdown of the classification developed for noninteracting systems [21]. In this Letter we study effect of interactions on the topological phase diagram using a realistic model which describes multiband nanowires proximity-coupled to an s-wave superconductor. The effective theory naturally emerging in multiband nanowires is equivalent to the model of two coupled Majorana chains. Rather than being spatially dependent, the coupling between Majorana "chains" is controlled by external parameters such as magnetic field and chemical potential. Within this model, we characterize the effect of interparticle interactions as well as various other perturbations on the topological phase diagram. We find that interactions do not change the phase diagram at the qualitative level but lead to a non-trivial renormalization of the phase boundary.

Theoretical model. The system we consider here consists of a semiconductor quantum well with dimensions $L_z \ll L_y \ll L_x$ in contact with an s-wave superconductor, see Fig.1a. We assume that the confinement along the z-axis is very strong so that only the lowest subband with respect to the z-axis eigenstates is occupied, whereas the confinement along the y-axis is much weaker and few a subbands in the y-direction can be populated. In the rest of the paper we consider an effective two-band model for the semiconductor nanowire which captures the physics we are interested in. Within this approximation, the Hamiltonian of the system reads ($\hbar = 1$):

$$H_{\rm SM} = \sum_{\lambda\lambda'} \int_{-L}^{L} dx \left[c^\dagger_\lambda \left(-\frac{\partial_x^2}{2m^*} - \mu + V_x\sigma_x + i\alpha\sigma_y\partial_x \right)_{\lambda\lambda'} c_{\lambda'} + d^\dagger_\lambda \left(-\frac{\partial_x^2}{2m^*} - \mu + E_{\rm sb} + V_x\sigma_x + i\alpha\sigma_y\partial_x \right)_{\lambda\lambda'} d_{\lambda'} \right]. \quad (1)$$

$$H_{\rm P} = \int_{-L}^{L} dx \left[\Delta_0 c^\dagger_\uparrow c^\dagger_\downarrow + \Delta_0 d^\dagger_\uparrow d^\dagger_\downarrow + h.c. \right]. \quad (2)$$

Here c_λ and d_λ represent fermion annihilation operators of the first and second subbands having spin λ; $E_{\rm sb}$ is the subband energy difference due to the transverse confinement. The parameters m^*, μ, and α are the effective mass, chemical potential, and strength of spin-orbit Rashba interaction, respectively, and $2L$ is the length of the wire, which is taken to be much longer than the effective superconducting coherence length ξ in the semiconductor. An in-plane magnetic field B_x leads to spin splitting of the bands at zero momenta $V_x = g\mu_B B_x/2$, where $g_{\rm SM}$ is the g-factor in the semiconductor and μ_B is the Bohr magneton. The Hamiltonian $H_{\rm P}$ describes the proximity effect due to electron tunneling across the semiconductor/superconductor interface. For simplicity, we assume that the induced superconducting pair potential is the same for the first and second transverse bands.

As shown in Ref. [22], the system described by the Hamiltonian $H_0 = H_{\rm SM} + H_{\rm P}$ realizes a non-trivial topological SC state in a suitable parameter regime. In the weak coupling limit $\Delta_0 \to 0$, the topological phase emerges when there is an odd number of Fermi surfaces. In this case, the Hamiltonian of the system is adiabatically connected with the one of a spinless p-wave superconductor which is known to host Majorana zero-energy modes at the ends of the nanowire. As shown in Fig. 1b, such a situation is realized when $|V_x| > |\mu|$ and $|V_x| > |\mu - E_{\rm sb}|$ which corresponds to the topological phases

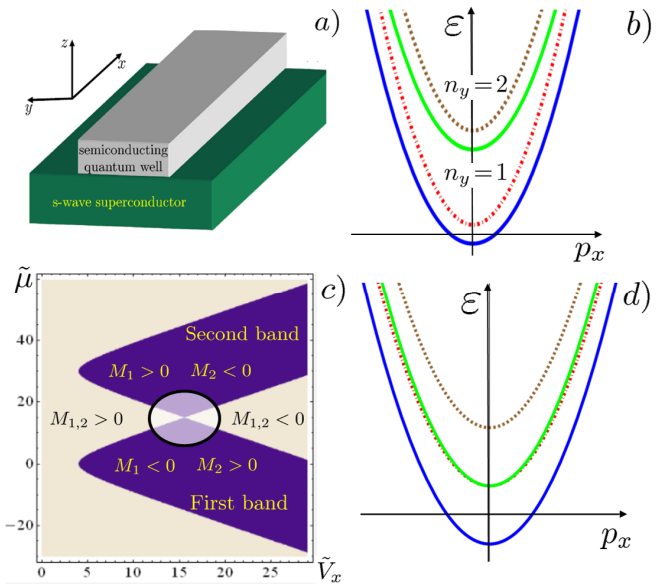

FIG. 1. (Color online) a) Semiconductor quantum well with dimensions $L_z \ll L_y \ll L_x$ in contact with an s-wave superconductor. b) Single-particle energy spectrum showing lowest two transverse subbands. The combination of the Rashba spin-orbit coupling and magnetic field results in splitting of the spin degeneracy in each subband. c) Phase diagram for two-band topological superconductor assuming fermion parity in each subband is conserved. At the multicritical point the system has enhanced $Z_2 \otimes Z_2$ symmetry and is equivalent to the model of two Majorana chains. Changing of the mass terms M_a corresponds to a topological phase transition and allows one to map out the topological phase diagram. Here tilde denotes rescaled energy $\tilde{E} \equiv E/m^*\alpha^2$. d) Single-particle energy spectrum at the multicritical point where two bands belonging to different subbands touch, and the band topology changes in a non-trivial way.

originating from the first ($n_y = 1$) and second ($n_y = 2$) subbands, respectively. Looking at the single-particle band structure as a function of V_x, one can notice that there is a special point $V_x \approx E_{\rm sb}/2$ where two bands belonging to $n_y = 1$ and $n_y = 2$ subbands touch, see Fig. 1c and d. If the chemical potential is tuned to $\mu = E_{\rm sb}/2$, the single particle band topology changes in a non-trivial way at this point (i.e. the first Chern number defined for two-band Bogoliubov-De Gennes Hamiltonian changes by 2) yielding an interesting phase diagram which is similar to two coupled Majorana chains. In this case, however, instead of originating from physically different chains, Majorana fermions emerge here from different transverse subbands. We first analyze the phase diagram assuming the fermion parity in each subband is preserved, and then discuss how various perturbations including interactions affect the topological phase diagram.

In the case of a fixed fermion parity in each subband, one can introduce a Z_2 topological invariant $\mathcal{M}$ (Majorana number) [20, 22] for each band $\mathcal{M}_1$ and $\mathcal{M}_2$. The change of the topological invariant signals the phase transition with the phase boundary given by $|V_x| = \sqrt{\mu^2+\Delta_0^2}$ and $|V_x| = \sqrt{(\mu-E_{\rm sb})^2+\Delta_0^2}$ for $n_y = 1$ and $n_y = 2$ subbands, respectively. At a special point in the phase diagram $\mu = E_{\rm sb}/2$ and $V_x = \sqrt{E_{\rm sb}^2/4+\Delta_0^2}$, two topological phases can coexist and the symmetry group is $Z_2 \otimes Z_2$, see Fig. 1c. Around this point there are four distinct phases: non-topological (no Majorana modes), topological with Majorana fermions originating either from $n_y = 1$ or $n_y = 2$ subbands, and the last one with two Majorana modes localized on each end, see Fig. 1c. Thus, multiband semiconductor nanowires are interesting from both a fundamental and a practical point of view as they offer a possibility to investigate interaction between various topological phases in a realistic experimental system.

From now on we focus on the multicritical point, and present a simple explanation of the topological phase transition by deriving an effective long wavelength model around it. The topological phase transition requires vanishing of the excitation gap in the system for the reconstruction of the energy spectrum to occur [3]. The quasiparticle excitation gap at the phase boundary vanishes as $E(p) \sim |p|$ [5], and, thus, one can understand the phase diagram by deriving an effective model in the spirit of $k\cdot p$ perturbation theory. The phase transition between various topological phases can be captured by studying the Dirac-like Hamiltonian with the mass term(s) M changing sign across the phase boundary, see Fig. 1c. We first calculate exact eigenstates around the multicritical point, and then evaluate small corrections due to the deviation of the physical parameters away from this point. Assuming that these terms are small compared to $\mu, \Delta_0, V_x \sim E_{\rm sb}$, we perform the following canonical transformation and project the system to a low energy subspace $\varepsilon \ll E_{\rm sb}$:

$$c_{\uparrow/\downarrow} \approx \pm u_-(e^{i\frac{\pi}{4}}\gamma_R^{(1)}+e^{-i\frac{\pi}{4}}\gamma_L^{(1)})+u_+(e^{-i\frac{\pi}{4}}\gamma_R^{(1)}+e^{i\frac{\pi}{4}}\gamma_L^{(1)}),$$
$$d_{\uparrow/\downarrow} \approx \mp u_+(e^{i\frac{\pi}{4}}\gamma_R^{(2)}+e^{-i\frac{\pi}{4}}\gamma_L^{(2)})-u_-(e^{-i\frac{\pi}{4}}\gamma_R^{(2)}+e^{i\frac{\pi}{4}}\gamma_L^{(2)}). \quad (3)$$

Here $\gamma_{R/L}^{(a)}$ are right/left-moving Majorana operators originating from the first ($a=1$) and second ($a=2$) subbands, respectively. In the transformation above we kept only low energy degrees of freedom and neglected high-energy modes. (Note, however, that these high-energy modes are necessary to satisfy canonical anticommutation relations.) The amplitudes $u_\pm$ are given by

$$u_\pm = \frac{1}{2\sqrt{2}}\frac{\sqrt{E_{\rm sb}^2+4\Delta_0^2 \pm E_{\rm sb}\sqrt{E_{\rm sb}^2+4\Delta_0^2}}}{\sqrt{(E_{\rm sb}^2+4\Delta_0^2)}}.$$

After some algebra, one arrives at the following effective Hamiltonian valid in the vicinity of the multicritical point:

$$H_0 \approx \sum_{a=1,2}\int_{-L}^{L} dx\left[i\tilde{\alpha}(\gamma_L^{(a)}\partial_x\gamma_L^{(a)}-\gamma_R^{(a)}\partial_x\gamma_R^{(a)})+iM_a\gamma_L^{(a)}\gamma_R^{(a)}\right], \quad (4)$$

where $\tilde{\alpha} = \alpha\Delta_0/\sqrt{E_{\rm sb}^2+4\Delta_0^2}$ and the mass terms M_a can be written in terms of the deviations from the multicritical point $\delta V_x = V_x - \sqrt{E_{\rm sb}^2/4+\Delta_0^2}$ and $\delta\tilde{\mu} = E_{\rm sb}(\mu -$

$E_{\rm sb}/2)/\sqrt{E_{\rm sb}^2+4\Delta_0^2}$:

$$M_{1/2}=-2\delta V_x\pm 2\delta\tilde{\mu}. \quad (5)$$

The topological phase transitions can be classified in terms of the sign change of the mass terms M_a, see Fig. 1c. It is clear that the phase with $M_{1,2}>0$ is trivial since it is adiabatically connected to $V_x=0$ limit. A sign change of one of the two mass terms corresponds to a topological transition to a phase with a single Majorana mode. Finally, when both mass terms change sign we have two Majorana modes per end. However, the latter state is unstable against perturbations that break fermion parity in the individual chain and ultimately lift the degeneracy by hybridizing the Majorana modes.

We consider below effect of the symmetry-breaking terms which couple Majorana modes $\gamma^{(1)}$ and $\gamma^{(2)}$ on the topological phase diagram. The presence of such terms reduces the $Z_2\otimes Z_2$ symmetry of the model introduced in Eq. (4) to Z_2 where the two phases corresponds to a different total fermion parity of the system [20]. Let us consider, for example, the interband superconducting pairing term

$$H_{\rm P}^{(12)}=\int_{-L}^{L}[\Delta_{12}(d_\uparrow^\dagger c_\downarrow^\dagger+c_\uparrow^\dagger d_\downarrow^\dagger)+h.c.]$$
$$\approx -2i\Delta_{12}\int_{-L}^{L}dx[\gamma_R^{(1)}\gamma_L^{(2)}-\gamma_L^{(1)}\gamma_R^{(2)}], \quad (6)$$

where in the last line we performed the canonical transformation (3) and projected the Hamiltonian into the low energy subspace. This term indeed couples Majorana fermions originating from different subbands, and, modifies the phase diagram at the qualitative level, see Fig. 2a. One can show that for $\delta\tilde{\mu}=0$ the energy spectrum of $H_0+H_{\rm P}^{(12)}$ becomes $E_\pm(p)=\sqrt{(\tilde{\alpha}p)^2+(\delta V_x\pm\Delta_{12})^2}$, and both Majorana modes become massive at the multicritical point. However, the excitation gap now vanishes at $\delta V_x=\pm\Delta_{12}$ indicating that there is a window $-|\Delta_{12}|<\delta V_x<|\Delta_{12}|$ where topological phases from different subbands coexist corroborating the results of Ref. [22]. For $\delta\tilde{\mu}\neq 0$, the phase boundary reads $\delta V_x=\pm\sqrt{\delta\tilde{\mu}^2+\Delta_{12}^2}$. As emphasized in Ref. [22], this effect is particularly important for experimental realization of the topological superconducting phase in semiconductor nanowires where chemical potential fluctuations pose serious constraint. Indeed, in this region the topological phase is to a large extent robust against chemical potential fluctuations which now have to be $\delta\mu\sim E_{\rm sb}$ to cause the transition into the nontopological state.

Interaction effects. We now study the effect of interactions on the topological superconducting phase. For simplicity, we consider short-range interactions given by the Hamiltonian

$$H_{\rm int}=U\sum_{\lambda,\lambda'=\uparrow,\downarrow}\int_{-L}^{L}dx:(c_\lambda^\dagger c_\lambda+d_\lambda^\dagger d_\lambda)::(c_{\lambda'}^\dagger c_{\lambda'}+d_{\lambda'}^\dagger d_{\lambda'}):$$
(7)
$$\approx-\tilde{U}\int_{-L}^{L}dx:(\gamma_L^{(1)}\gamma_R^{(1)}-\gamma_L^{(2)}\gamma_R^{(2)})::(\gamma_L^{(1)}\gamma_R^{(1)}-\gamma_L^{(2)}\gamma_R^{(2)}),$$

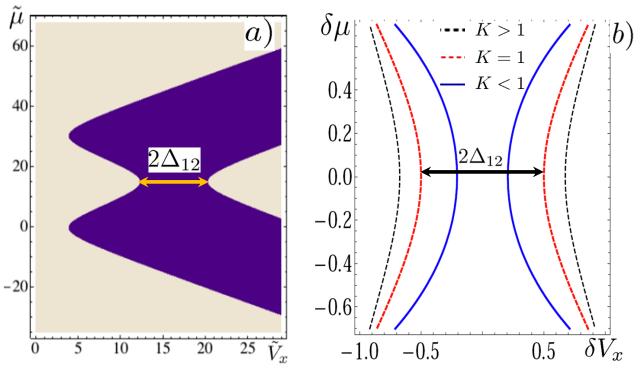

FIG. 2. (Color online) a) Topological phase diagram for two band semiconductor model in the presence interband superconducting pairing Δ_{12} which breaks fermion parity in the individual subband and leads to the hybridization between the Majorana modes originating from $n_y=1$ and $n_y=2$ subbands. As a result, the enhanced $Z_2\otimes Z_2$ symmetry at the multicritical point is broken down to Z_2, compare with Fig 1c. b) Shift of the topological phase boundary caused by interactions. Repulsive/attractive interaction lead to the suppression/enhansement of the topological phase at the multicritical point.

where $\tilde{U}=U\frac{E_{\rm sb}^2}{E_{\rm sb}^2+4\Delta_0^2}$. In the last line of Eq. (7) we have projected the Hamiltonian to the low energy subspace. Combining all the terms, the full Hamiltonian for the interacting system becomes $H=H_0+H_{\rm P}^{(12)}+H_{\rm int}$. One can see that at the multicritical point (assuming $\Delta_{12}=0$), the Hamiltonian H maps onto Thirring model which can be solved exactly using bosonization. Note that the interaction term (7) does not break fermion parity in the individual chain, and preserves $Z_2\otimes Z_2$ symmetry present at the multicritical point. The effect of deviations from the multicritical point as well as effect of symmetry-breaking terms can be included in the model perturbatively assuming that these terms are small. We proceed using standard bosonization [23] by first introducing left and right-moving Dirac fermions $\psi_{R/L}=(\gamma_{R/L}^{(1)}-i\gamma_{R/L}^{(2)})/\sqrt{2}$, and then rewriting them in terms of the bosonic fields φ and θ: $\psi_{R/L}\sim e^{i(\varphi\pm\theta)}$. The bosonized Hamiltonian H becomes

$$H=\frac{v}{2\pi}\int_{-L}^{L}dx\left[K(\partial_x\varphi)^2+\frac{1}{K}(\partial_x\theta)^2-\frac{2y_1}{a^2}\sin 2\theta-\frac{2y_2}{a^2}\cos 2\varphi\right], \quad (8)$$

where the v, K, $y_{1,2}$ are related to the microscopic parameters of the model: $v=2\tilde{\alpha}\sqrt{1-\left(\tilde{U}/\pi\tilde{\alpha}\right)^2}$, $K=\sqrt{(1-\frac{\tilde{U}}{\pi\tilde{\alpha}})/(1+\frac{\tilde{U}}{\pi\tilde{\alpha}})}$, $y_1=2\delta V_x a/v$, and $y_2=2\sqrt{\Delta_{12}^2+\delta\tilde{\mu}^2}a/v$. Here a is a cutoff in the problem, which is related to the momentum bandwidth $\Lambda\sim 1/a$ [23]. Note that at $K=1$ and $y_1=y_2$ the model is self-dual $\varphi\leftrightarrow\theta$. We note in passing that the Hamiltonian (8) appears in other systems such as classical two-dimensional XY model in a magnetic field and weakly coupled Heisenberg chains, see, e.g.

Refs. [24–26], and one can develop some intuition based on these analogies.

We now investigate how interactions modify the topological phase diagram of the system and study effects of the competing relevant operators on the non-trivial criticality. Assuming that $y_{1,2} \to 0$, one can obtain flow equations using a perturbative real-space RG approach [25]:

$$\frac{dy_1(l)}{dl} = (2-K)y_1(l), \tag{9}$$

$$\frac{dy_2(l)}{dl} = (2-K^{-1})y_2(l), \tag{10}$$

$$\frac{d\ln K}{dl} = K^{-1}y_2^2 - Ky_1^2, \tag{11}$$

where $l = \ln[a/a_0]$ is the flow parameter with a_0 being the initial value of the cutoff. As one can see in the vicinity of $K = 1$, where we have a non-trivial critical point, both mass terms are relevant and flow to strong coupling under RG, i.e. each perturbation acting separately would yield a massive field theory. However, given that y_1 and y_2 couple to dual field operators corresponding to charge-density-wave pairing and Cooper-pairing, respectively, and drive the system to different ground states, the interplay between them gives rise to a second-order phase transition at intermediate coupling. Indeed, this is what happens at the self-dual point $K=1$. Away from this exactly solvable point, some intuition can be obtained by invoking scaling arguments. Using the analogy with 2D classical theory, the scaling theory of our zero-temperature 1D problem can be easily formulated. Since the critical theory should be invariant under the rescaling, the singular part of the energy density satisfies the following scaling relations:

$$f_s[y_1, y_2] = e^{-2l} f_s[e^{(2-K)l}y_1, e^{(2-K^{-1})l}y_2]. \tag{12}$$

The scale l can be fixed by requiring $e^{(2-K^{-1})l^*}y_2 = 1$. Substituting l^* into the energy density, one finds

$$f_s[y_1, y_2] = y_2^{\frac{2}{2-K^{-1}}} f_s\left[y_2^{-\frac{2-K}{2-K^{-1}}}y_1, 1\right]. \tag{13}$$

The phase transition in this system occurs when $y_2^{-\frac{2-K}{2-K^{-1}}}y_1 \sim 1$, and, thus, the new phase boundary is given by

$$\delta V_x = \pm\left(\Delta_{12}^2 + \delta\mu^2\right)^{\frac{1}{2}\frac{2-K}{2-K^{-1}}}. \tag{14}$$

This is one of the main results of the paper. The presence of interactions does not modify the multicritical point but leads to a non-trivial renormalization of the phase boundary which now depends on the Luttinger liquid parameter K. One can easily see that Eq. (14) is consistent with the noninteracting ($K = 1$) result discussed earlier. In the case of a repulsive interaction ($K<1$), the topological region at the multicritical point shrinks, see Fig. 2b. This result can be understood as a competition between the repulsive interaction and proximity-induced superconductivity, and in this regard, our conclusions are consistent with those of Refs. [27, 28]. On the contrary, attractive interaction ($K>1$) stabilizes the topological phase by expanding the area occupied by the topological phase, see Fig. 2b.

To conclude, we have studied interacting topological superconducting phases using a realistic model corresponding to the semiconductor nanowire in the limit of multiband occupancy in contact with an s-wave superconductor. In the vicinity of the multicritical point in the phase diagram, the model considered here is equivalent to the one describing two coupled Majorana chains, and we have characterized the effect of interactions as well as other perturbations on the topological phase diagram. We find that moderate interactions do not affect the phase diagram qualitatively but lead to nontrivial quantitative changes in the phase boundary. Our results characterize the stability of the topological phase around the multicritical point against interactions and have important implications for the experiments on Majorana nanowires.

Acknowledgements. We would like to thank J. Alicea, F. Essler, P. Fendley, E. Fradkin, L. Fidkowski, and C. Nayak for enlightening discussions.

[1] B. G. Levi, Physics Today **64**, 20 (2011).
[2] F. Wilczek, Nature Physics **5**, 614 (2009).
[3] N. Read and D. Green, Phys. Rev. B **61**, 10267 (2000).
[4] D. A. Ivanov, Phys. Rev. Lett. **86**, 268 (2001).
[5] J. Alicea, Y. Oreg, G. Refael, F. von Oppen, and M. P. A. Fisher, Nature Physics (2011), doi:10.1038/nphys1915.
[6] C. Nayak, S. H. Simon, A. Stern, M. Freedman, and S. Das Sarma, Rev. Mod. Phys. **80**, 1083 (2008)
[7] J. D. Sau, R. M. Lutchyn, S. Tewari, and S. Das Sarma, Phys. Rev. Lett. **104**, 040502 (2010).
[8] J. Alicea, Phys. Rev. B **81**, 125318 (2010).
[9] R. M. Lutchyn, J. D. Sau, and S. Das Sarma, Phys. Rev. Lett. **105**, 077001 (2010)
[10] Y. Oreg, G. Refael, and F. von Oppen, Phys. Rev. Lett. **105**, 177002 (2010).
[11] J. Nilsson, A. R. Akhmerov, and C. W. J. Beenakker, Phys. Rev. Lett. **101**, 120403 (2008).
[12] L. Fu and C. L. Kane, Phys. Rev. B **79**, 161408 (2009).
[13] L. Fu, Phys. Rev. Lett. **104**, 056402 (2010).
[14] K. T. Law, P. A. Lee, and T. K. Ng, Phys. Rev. Lett. **103**, 237001 (2009).
[15] J. D. Sau, S. Tewari, R. M. Lutchyn, T. D. Stanescu, and S. Das Sarma, Phys. Rev. B **82**, 214509 (2010).
[16] F. Hassler, A. R. Akhmerov, C.-Y. Hou, and C. W. J. Beenakker, New Journal of Physics **12**, 125002 (2010).
[17] J. D. Sau, S. Tewari, and S. Das Sarma, Phys. Rev. A **82**, 052322 (2010).
[18] P. Bonderson and R. M. Lutchyn, Phys. Rev. Lett. **106**, 130505 (2011).
[19] L. Fu and C. L. Kane, Phys. Rev. Lett. **100**, 096407 (2008)
[20] A. Y. Kitaev, Physics-Uspekhi **44**, 131 (2001)
[21] L. Fidkowski and A. Kitaev, Phys. Rev. B **81**, 134509 (2010).
[22] R. M. Lutchyn, T. D. Stanescu, and S. Das Sarma, Phys. Rev. Lett. **106**, 127001 (2011).

[23] T. Giamarchi, *Quantum physics in one dimension* (Oxford University Press, 2004).
[24] P. Lecheminant, A. O. Gogolin, and A. A. Nersesyan, Nuclear Physics B **639**, 502 (2002).
[25] J. V. José, L. P. Kadanoff, S. Kirkpatrick, and D. R. Nelson, Phys. Rev. B **16**, 1217 (1977).
[26] H. A. Fertig, Phys. Rev. Lett. **89**, 035703 (2002).
[27] S. Gangadharaiah, B. Braunecker, P. Simon, and D. Loss, ArXiv e-prints (2011), arXiv:1101.0094 [cond-mat.str-el].
[28] E. Sela, A. Altland, and A. Rosch, ArXiv e-prints (2011), arXiv:1103.4969 [cond-mat.str-el].